

Metal-halide lamps in the international space station ISS

Abstract. Optical emission spectroscopy was performed on a metal-halide lamp under the micro-gravity conditions of the international space station (ISS). Several transitions of atomic and ionic Dy, and atomic Hg have been measured at different lateral positions from which we obtained atomic and ionic Dy and atomic Hg intensity profiles. After Abel inversion, the calibrated radial intensity profile of Hg was used to calculate a radial temperature profile. By combining the radial temperature profile with the calibrated radial intensity profile of the additive, the absolute radial density profile of the total atomic and ionic density of Dy was obtained. The measurements showed a hollow density profile for the atoms and ions in the centre. In the outer parts of the lamp molecules were found to dominate. Lamps containing Dy showed contraction of the arc, which increased for higher powers. Measurements were duplicated at 1-*g* and showed less radial segregation than for 0-*g*. As the power was increased, the difference between 0-*g* and 1-*g* of the radial intensity, density and temperature profile were diminished.

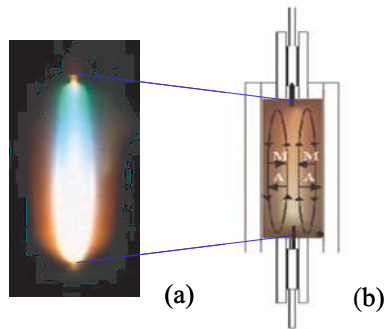


Figure 3.1: (a) Colour separation in a metal-halide lamp burner. (b) Schematic view of a metal-halide lamp; diffusion and convection of atoms (A) and molecules (M) are indicated by arrows. See figure 1.1 for full colour.

3.1 Introduction

The need for compact high-intensity light sources with high luminous efficacy and good colour rendering properties has led to the development of the metal-halide lamp [1]. This type of arc lamp contains a buffer gas of Hg and a relatively small amount of a mixture of additives such as DyI_3 , CeI_3 or NaI salts, which supply the prime radiators. More than two salt components are necessary for a good colour rendering index, therefore mixtures such as $(\text{NaI} + \text{ScI}_3)$, $(\text{NaI} + \text{TlI} + \text{InI})$ or $(\text{NaI} + \text{TlI} + \text{DyI}_3 + \text{HoI}_3 + \text{TmI}_3)$ are commonly used in metal-halide lamps.

Due to the competition between diffusive and convective processes these additives are non-uniformly distributed over the lamp, resulting in the undesirable segregation of colours [2], see figure 3.1. This means that lamp performance is strongly dependent on burning orientation (vertical and horizontal). Since the convective processes are induced by gravity, placing the arc lamp in a gravity-free environment would aid the understanding of the transport processes resulting in this so-called de-mixing. Previous efforts to observe the arc and its characteristics in micro-gravity include the relatively straightforward emission measurements aboard the space shuttle [3] [4], and the optical emission spectroscopy measurements during the parabolic flights [5] [6]. During the parabolic flights, however, micro-gravity was obtained for a period of only 20 to 25 seconds. This is not enough time for the arc to adjust to the micro-gravity conditions. The international space station (ISS), on the other hand, provides a gravity-free environment where stable arc conditions are ensured.

In this paper we present and discuss experiments performed on HID lamps in the ISS in 24th and 25th April in 2004 by André Kuipers. There the lamps were subjected to extended micro-gravity conditions in order to separate and help clarify the role of convection and other transport mechanisms in the arc of the lamp. For the purpose of this study the lamp was filled with an Hg buffer gas and one salt, namely DyI_3 . This lamp has a relatively simple salt system and therefore the results are easier to compare with the results of a numerical

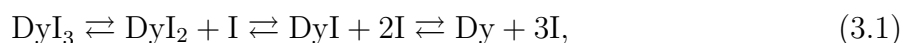
model. For comparison, lamps containing pure Hg were also studied. The lamp was investigated by means of optical emission spectroscopy, which yields line intensities of the species Hg and Dy [7]. From calibrated Hg line intensity we constructed radial temperature profiles. By combining the temperature profile with the calibrated line intensities for Dy we obtained absolute radial density distributions for these species. All measurements were done for different powers ranging from 70 to 150 W.

This chapter is organized as follows. Section 3.2 describes the segregation phenomenon and the method used to determine the temperature of the arc and atomic and ionic densities. Section 3.3 describes the arc lamps used in the experiments and the experimental setup. Results from the experiments are presented and discussed in section 3.4. These results constitute radial profiles of the arc temperature and absolute atomic and ionic densities of Dy for different lamp powers. Finally, section 3.5 offers conclusions and recommendations for future work.

3.2 Theory

3.2.1 Segregation

The main light emitting species, Dy atoms and ions, are brought into the plasma by evaporation of the liquid DyI_3 , molecules of which then dissociate into atoms and ions. Whereas the Hg evaporates completely, the few milligrams of the DyI_3 additive do not entirely evaporate, leaving a liquid salt pool at the coldest spot of the burner wall. The cold spot determines the vapour pressure of the additive in the immediate vicinity of the salt pool. Because of the large temperature gradient between the wall (~ 1200 K) and the centre of the burner (~ 6000 K) [8], a multi-step process of dissociation of DyI_3 molecules towards the centre and association of atoms into molecules near the wall takes place. The reaction balances chain can be described as follows,



the temperature increasing to the right. At the hot centre Dy atoms ionize and Dy ions are created,



Three mechanisms influence the distribution of particles in the plasma. First, there is a high temperature in the centre, which rapidly decreases towards the wall. Because of $p = nkT$ this high temperature results in a hollow profile of the density distribution over the lamp. Second, there is the difference between the diffusion velocities of atoms and molecules. The smaller and lighter Dy atoms diffuse faster outward than the larger and heavier molecules (DyI , DyI_2 , DyI_3) diffuse inward. This difference in diffusion velocity results, in steady-state, in an even more hollow profile of the elemental density of Dy; this is called radial segregation [2]. Elemental density is defined as the density that contains all molecular, atomic and ionic contributions of a particular element.

The third mechanism, convection, causes the hot gas to move upwards in the hot centre of the arc and downwards along the cool wall of the lamp. This movement of the bulk gas drags the high concentration of Dy near the wall downwards. Whereas, the lower concentration of Dy in the centre, caused by the radial segregation, is dragged upwards. As a consequence, high density of elemental Dy accumulates at the bottom of the arc, a phenomenon which is known as axial segregation [2]. The combination of axial and radial segregation is shown in figure 3.1(b).

One way to study radial segregation of Dy exclusively is to prevent the formation of axial segregation. By placing the metal-halide lamp in a gravity-free environment, no convection can take place and therefore no axial segregation occurs. This gravity-free environment is realised in the international space station ISS.

In most HID lamps, the discharge contracts toward the axis of the arc tube, creating a dark annular space between the discharge and the tube wall [9]. The gas temperature profile in such a contracted discharge can be described by an expression proposed by Fischer for high pressure discharges [10]

$$T(r) = T_{wall} + T_1 \left(1 - \left(\frac{r}{R}\right)^2\right) + T_2 \left(1 - \left(\frac{r}{R}\right)^2\right)^\gamma, \quad (3.3)$$

with r the radius and R the total radius of the arc tube, γ is a measure for the amount of contraction of the discharge. T_1 and T_2 are fitting parameters that determine the maximum temperature in the centre of the discharge ($r=0$), together with the value of γ . The wall temperature T_{wall} is estimated to be about 1200 K at the midplane of the lamp [8] that was investigated in this study.

3.2.2 Emission of radiation

One way to study the effect of radial segregation is to determine the radial density profiles of the additives. If the discharge is in LTE (Local Thermal Equilibrium), the density of the additives can be determined by measuring the intensity of light emitted by atoms and ions.

For an optically thin line, the radiant power U_{pq} [Wm^{-3}] emitted by a spectral line is

$$U_{pq} = A(p, q) h\nu_{pq} n_p, \quad (3.4)$$

where $A(p, q)$ is the transition probability of the transition, $h\nu_{pq}$ the energy of the emitted photon, and n_p the number density of an emitting atom or ion in upper energy level p . Under LTE conditions, the Boltzmann relation [11] can be used to link the number density n_p to the total number (system) density n_s of the atom or ion

$$n_p = n_s \frac{g_p}{Q(T)} \exp\left(\frac{-E_p}{kT}\right), \quad (3.5)$$

where g_p is the statistical weight of upper level p , T is the temperature and k the Boltzmann constant. $Q(T)$ is the partition function of the considered atomic or ionic system

$$Q(T) = \sum_i g_i \exp\left(\frac{-E_i}{kT}\right). \quad (3.6)$$

We can now determine the total number density of particles of a particular atomic system from the radiant power

$$n_s = \frac{U_{pq}Q(T)}{g_p A(p, q) h \nu_{pq}} \exp\left(\frac{E_p}{kT}\right), \quad (3.7)$$

where U_{pq} is determined experimentally, while $Q(T)$, g_p , $A(p, q)$ can be found in literature [12–14]. What is needed for the calculation of the density using equation (3.7) is the radially resolved radiant power $U_{pq}(r)$, which is acquired by the line intensity measurement of the optically thin line of the species in question, and the arc temperature $T(r)$ as a function of radial position.

The radiant power $U_{pq}(r)$ of an optically thin line is deduced from the lateral (i.e. line-of-sight) measurement of the arc. The wavelength integrated intensity of the chosen spectral line is determined as a function of lateral position. This yields the lateral intensity profile. A lateral profile constitutes the integrated spectral line intensity as a function of lateral position. Radial information can be extracted from a set of lateral measurements by the Abel inversion technique [15]. The technique used approximates the radial intensity profile j_{pq} by means of a polynomial series [16],

$$j_{pq}(r) = a_0 + \sum_{n=2}^{\infty} a_n r^n. \quad (3.8)$$

The term a_{1r} is omitted because, due to symmetry, the derivative of the dysprosium density at the axis of the burner should be zero. By applying a least-squares-fitting procedure to the lateral profile, the coefficients a_n are obtained and a radial profile is constructed [7]. In this way the lateral intensity profile is converted into the radial intensity profile which, after calibration, yields $U_{pq}(r)$.

The radial temperature profile is calculated from the dominant species, in this case atomic Hg. The temperature is calculated using equation (3.7), for which $U_{pq}(r)$ and the total Hg density n_{Hg} are needed. $U_{pq}(r)$ is determined from the optically thin 579 nm Hg line, which is calibrated. The total Hg density n_{Hg} can be reformulated in terms of temperature using the ideal gas law $p = nkT$, assuming $p = p_{\text{Hg}}$ and is constant over the discharge, where p_{Hg} can be written as

$$p_{\text{Hg}} = n_{\text{Hg}} kT_{\text{eff}} = \frac{N_{\text{Hg}} kT_{\text{eff}}}{V} = \frac{m_{\text{effHg}} N_A kT_{\text{eff}}}{m_{\text{Hg}} \pi R^2 h}. \quad (3.9)$$

N_A is Avogadro's number, m_{Hg} the molar mass of Hg; and R and h the total radius and height of the burner respectively. N_{Hg} is the total amount of Hg in the discharge region,

and T_{eff} is the effective temperature. m_{effHg} is the total Hg dose in the discharge region, this is defined as the burner volume minus the electrode volume (the volume behind the tip of the electrodes). We need to take into account the amount of Hg which is located behind the electrodes. This is estimated to be $38 \pm 10\%$, the effective Hg dose is therefore estimated to be 62% of the total Hg dose [17]. The effective temperature T_{eff} can be calculated using

$$T_{eff} = \frac{p_{Hg}V}{N_{Hg}k} \quad (3.10)$$

which can be rewritten using

$$N_{Hg} = \int n_{Hg}dV = \frac{p_{Hg}}{k} \int \frac{1}{T(r)}dV. \quad (3.11)$$

Assuming cylinder-symmetry and combining equations (3.10) and (3.11), the effective temperature can now be written as

$$T_{eff} = \frac{V}{\int \frac{1}{T(r)}dV} = \frac{R^2}{2 \int_0^R \frac{r}{T(r)}dr}. \quad (3.12)$$

Combined with equation (3.7), $T(r)$ can be calculated numerically from the measured $U_{pq}(r)$ of the 579 Hg line using an iterative method. The 579 nm Hg line cannot, however, be accurately determined at radial positions beyond $r > 2$ mm. Therefore, the temperature profile is extrapolated using the expression for the radial temperature profile introduced by Fischer [10]. This expression is used to extrapolate the temperature from the inner part of the burner to the wall. The error in the temperature profile is estimated to be less than 10% over the whole range.

3.3 Experimental Setup

The spectrometer, used for the optical emission measurements of HID lamps, was exclusively designed for measurements in the ISS [18]. Accordingly, the spectrometer had to be compact, light weight, and robust. Ordinary spectrometers make use of the accurate movement of a dispersion grating for wavelength selection and are therefore not suitable for an experiment in space. They also tend to be relatively large, as large focal lengths are needed for the lenses in order to achieve a reasonable spectral resolution. The requirement for compactness is solved by using an Echelle grating with a high blaze angle (74°). Due to the high angle of incidence and the use of high orders, the dispersion is high and therefore the focal length of the lenses can be relatively small, allowing the spectrometer to be very compact. A disadvantage of Echelle-type spectrometers is that they have a relatively small free spectral range (FSR) at high orders, which results in wavelength overlapping of adjacent orders at a fixed position on the detector. By placing an interference filter in the optical system for the selection of a small wavelength interval, the problem of overlapping orders is avoided. As different filters can be selected for different wavelength intervals,

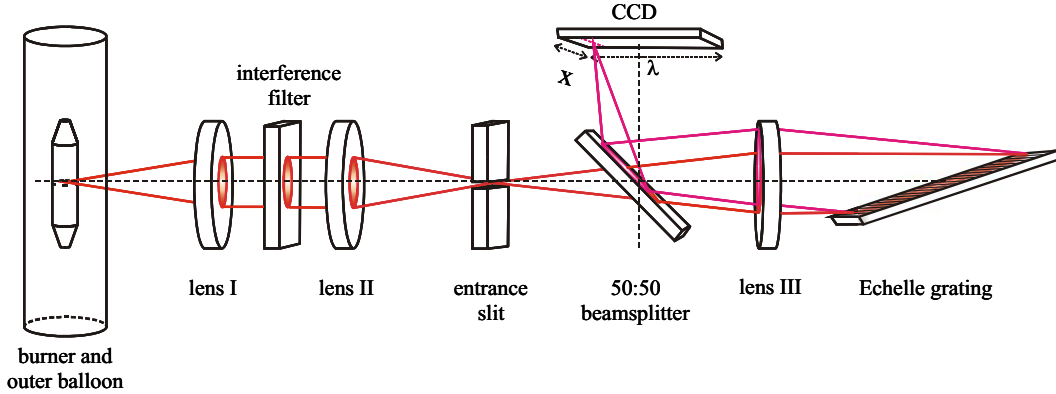


Figure 3.2: Setup used for the ISS measurements. It is an Echelle type spectrometer in Littrow configuration, the imaging lens (III) is used for the collimation of both the un-dispersed beam of light as well as the reflected dispersed beam of light.

the angle of the grating remains fixed. In this way, the requirement for robustness is also fulfilled, because no critically moving parts exist inside the spectrometer [18].

In the ISS experiment, emission spectroscopy was performed on a metal-halide lamp [16]. The lamp consists of a quartz burner of 20 mm in length and 8 mm in inner diameter and a transparent quartz vacuum outer bulb. The burner is made of quartz in order to make the arc optically accessible. The distance between the electrodes is approximately 18 mm. Table 3.1 shows the used lamps with the different dosages. It is driven by a Philips Dynavision ballast with a 83 Hz square wave current profile, and operated at different input powers ranging from 70 to 150 W in steps of 20 W.

Hg dose (mg)	additive	additive dose (mg)
10.00	DyI ₃	4.044
5.00	DyI ₃	4.011
10.00	-	0
10.00	DyI ₃	4.128
5.00	DyI ₃	3.953
10.00	-	0

Table 3.1: Lamps with dosages of Hg and the additive DyI₃. All lamp burners are shaped as cylinders.

A schematic of the Echelle-type spectrometer is shown in figure 3.2 [17] [18]. The light originating from the plasma forms a parallel beam after going through lens I (100 mm focal distance). A parallel beam is necessary for the proper functioning of the wavelength selection by the interference filter, which is situated between lens I and lens II (also 100 mm focal distance). Lens I and II combined with the interference filter form a 1:1 image of the burner on the horizontally placed entrance slit (10 mm x 10 μ m) of the desired

wavelength interval. The light emanating from the slit is the emission along the cross-section at the centre of the burner. It passes a 50:50 beam splitter and after being collimated by an achromatic doublet (Lens III), the light reaches the Echelle grating (96 mm x 46 mm) having 79.01 lines/mm and a 74.1° blaze angle. Lens III is positioned at its focal distance (150 mm) from the entrance slit to create a parallel beam of light on the Echelle grating. Then the light is back-reflected and dispersed with conservation of the spatial information. The angle of the reflected light with the optical axis of the system depends on the wavelength of the light. The reflected light is collimated by the same doublet (Lens III) and focused via the 50:50 beam splitter on the CCD-surface of the camera (SBIG ST-2000XM, 1600x1200 pixels of $7.4\mu\text{m}$ x $7.4\mu\text{m}$). As the wavelength dispersion is in the horizontal direction, we obtain a complete lateral profile in one measurement. The two-dimensional CCD image therefore contains the lateral cross-section in the vertical direction of the lamp, measured at a position halfway between the two electrodes. In the horizontal direction the CCD image contains the wavelengths of different atomic and ionic transitions. As stated before, wavelength selection is done by selecting the interference filter that corresponds to the desired wavelength interval [18].

Only the intensity of the 579 nm Hg line was calibrated with the ISS setup, using a source with known spectral radiance. Lamp L05, which contains only Hg, was measured on earth with the Echelle spectrometer with the interference filter corresponding to the 579 nm line, and calibrated with a Tungsten ribbon lamp. The lines that were used are listed in table 3.2. After the experiments were completed, calibration of the 402 and the 642 nm Dy lines were done with a setup nearly identical to the ISS setup [19] at 1g using, again, a Tungsten ribbon lamp. This allowed for the calibration of the Dy lines which were then used to calculate the absolute density of atomic and ionic Dy.

species	line (nm)	A value	source A value
Dy I	642.19	$1.6 \times 10^5 \text{ s}^{-1}$	Kurucz
Dy II	402.44	$8.4 \times 10^6 \text{ s}^{-1}$	Wickliffe and Lawler
Hg I	579.07	$2.1 \times 10^7 \text{ s}^{-1}$	Derived from Benck and Lawler

Table 3.2: Lines measured with the Echelle spectrometer. *A* values used for the calculation of the density of atoms and ions of Dy, and Hg, are taken from Kurucz [12] and Wickliffe, Benck and Lawler [13]. The *A* value for the 579.07 nm Hg line is derived from the $g_p A$ value for the 576.96 nm line [20]. The intensity of the 579.07 nm line is 10% lower than that of the 576.96 nm line and both lines have nearly the same upper level. The $g_p A$ value of the 579.07 nm line is therefore taken as 10% less than that of the 576.96 nm line. With $g_p=5$ this gives an *A* value of $2.1 \times 10^7 \text{ s}^{-1}$ for the 579.07 nm line.

Calculation of the radial density profiles of the additive Dy is as follows. First the emission of the line of interest is measured as a function of lateral position. The total intensity of the line is then calculated, which yields the lateral intensity profile. This profile is then Abel inverted into a radial intensity profile. The next step depends on the species of which the emission line is measured.

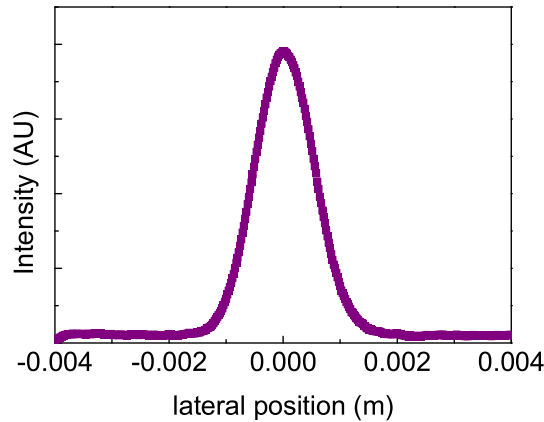


Figure 3.3: Lateral intensity profile of Hg at zero- g for a lamp containing 4 mg of DyI_3 and 10 mg of Hg operated at 150W.

In case of the 579 nm line of Hg, the intensity is calibrated and then the absolute radial intensity profile is used to numerically determine the temperature profile. If atomic or ionic lines of Dy are measured, the temperature profile is combined with the calibrated radial intensity profile of the additive into an absolute radial density profile as in equation (3.7).

3.4 Results and Discussion

In figure 3.3 the lateral intensity profile of atomic Hg is shown. The centre of the profile was determined by a parabolic fit, the maximum of which indicated the centre of the arc. Once the position of the centre was established, the Abel inversion technique was applied to transform the lateral intensity profile into a radial intensity profile of Hg. A typical result is given in figure 3.4.

After calibration, the radial intensity profile of Hg was used to calculate the temperature profile numerically, as described in the section 3.2.

Temperature profiles of a lamp containing 10 mg of Hg without Dy, are plotted for different lamp powers in figure 3.5. The temperature profile resembles a parabolic profile with a core temperature of about 5800 K for a lamp operated at 150W. The figure clearly shows that for increasing powers the temperature profile becomes broader.

Figure 3.6 shows the different lateral distributions of atomic and ionic species of Dy. The figure shows that ions are at the centre, surrounded by atoms. The atoms, in turn are surrounded by (non-detectable) molecules near the wall.

The lateral intensity profile for Dy does not go to zero near the edge of the arc, this is most probably caused by stray-light. In order for the Abel-fit to yield physical results, the fit was forced to zero near the edges of the lateral profile. Instead of covering the whole

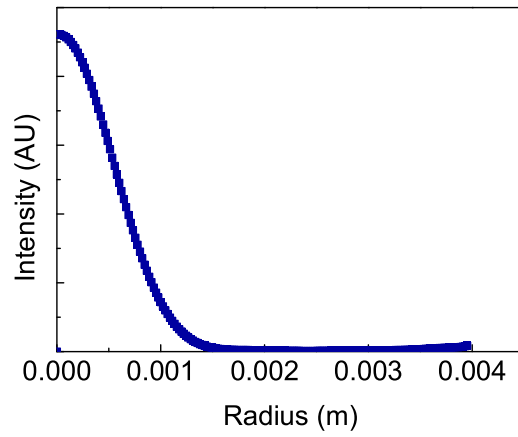


Figure 3.4: Radial intensity profile of Hg at zero- g for a lamp containing 4 mg of DyI_3 and 10 mg of Hg operated at 150W.

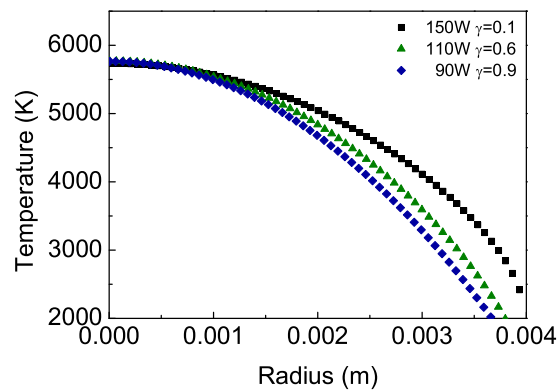


Figure 3.5: Radial temperature profiles at zero- g for a lamp containing 10 mg of Hg operated at different lamp powers. γ indicates the amount of contraction; $\gamma=1$ means there is no contraction. [10]

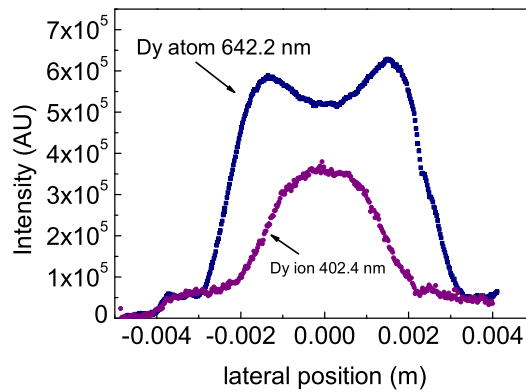


Figure 3.6: Lateral intensity profile of Dy at zero- g for a lamp containing 4 mg of DyI_3 and 10 mg of Hg operated at 150W.

range of the lateral profile (which is 8 mm wide), a slightly smaller fitting range (of about 6 mm wide) was chosen. This was done because atomic and ionic intensities are expected to go to zero near the wall, see figure 3.7. This caused a discrepancy in the fit near 3 mm, which was exacerbated by the exponent in the density calculation. The resulting density profile is therefore considered unreliable for $r > 3$ mm. Some of the density and intensity plots of Dy in this paper are therefore marked with a shaded area indicating the limit to which the plot can still be considered reliable.

From the lateral intensity profile, the radial intensity profile of atomic and ionic Dy (as shown in figure 3.8), was then constructed using the Abel inversion technique. To determine the total density of Dy atoms and ions, a radial temperature profile is required to be constructed for the lamp in question.

A typical example of a radial temperature profile of a lamp containing 10 mg of Hg and 4 mg of DyI_3 for different lamp powers is shown in figure 3.9. The axis temperature was about 6300 K for 150 W. It is clear that the arc contracted, especially at high powers such as 150W. The contraction can be quantitatively represented by the contraction parameter γ from equation 3.3. If $\gamma > 1$, the arc column is contracted. It was observed that $\gamma=0.1$ for a lamp operating at 150W with a pure Hg content, whereas for a lamp containing both Hg and Dy it was found that $\gamma=3.4$. Dy atoms are the main species responsible for radiation. Therefore, emission from the peripheral atomic Dy lines caused radiation loss at the flanks of the discharge, causing the arc to contract. The lamp was kept at constant power as the arc contracted, while the same amount of power went through a smaller volume. Therefore, if the radiation loss is small enough, the contraction caused the temperature to increase. When the power is increased the arc becomes more contracted, as more atomic Dy enters the arc, leading to an increase of radiation loss in the flank.

Combining the calibrated radial intensity profile with the radial temperature profile shown in figure 3.9, and using equation 3.7 we can calculate the radial density profile of

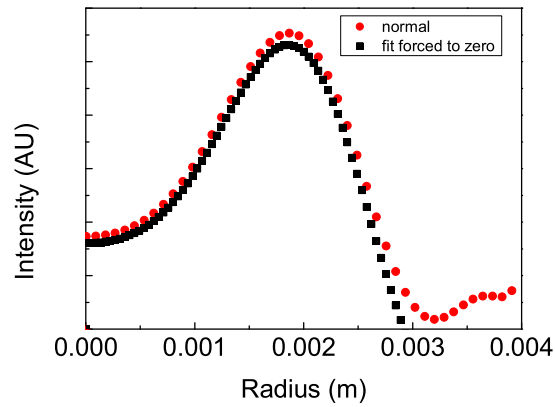


Figure 3.7: Two different Abel-fits at zero- g for a lamp containing 4 mg of DyI_3 and 10 mg of Hg operated at 150W. One fit is forced to zero near the edges of the lateral profile.

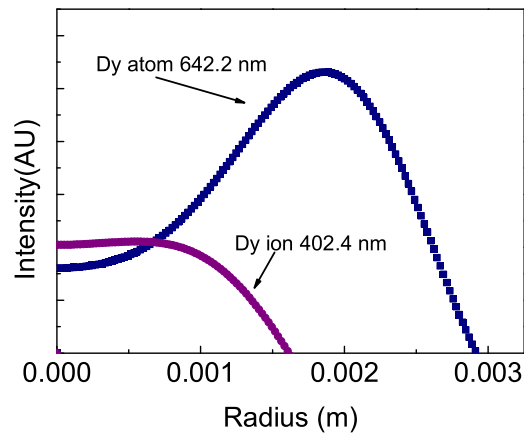


Figure 3.8: Relative radial intensity profile at zero- g for a lamp containing 4 mg of DyI_3 and 10 mg of Hg operated at 150W.

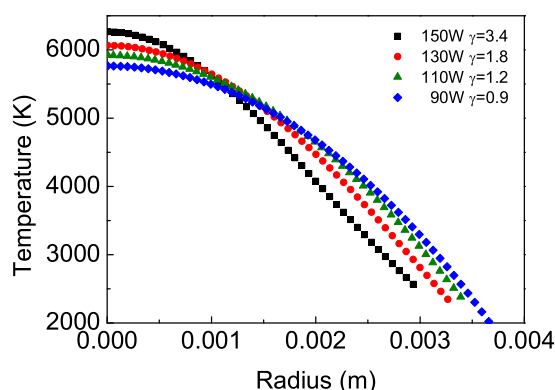


Figure 3.9: Radial temperature profiles at zero- g for a lamp containing 4 mg of DyI_3 and 10 mg of Hg operated at different lamp powers. γ indicates the amount of contraction, $\gamma=1$ means there is no contraction. [10]

the total atom or ion density. The radial density profiles of the total atom and ion Dy density are shown in figures 3.10 and 3.11 respectively. Dy atoms ionize into Dy ions in the hot centre of the lamp, causing a depletion of Dy atoms. The atomic density decreases toward the cooler wall making room for molecules. The contraction seen in the temperature profile can also be seen in these figures.

In order to determine which species dominated in the centre of the lamp, the ratio of Hg^1 and Dy ions has been calculated for a lamp operated at 150 W. The ratio of Hg^+/Dy^+ ions is shown in figure 3.12 as a function of the radius; it demonstrates that Hg ions are more abundant than the Dy ions up to $r = 1.5$ mm. In newer types of HID lamps, the burner is often made of PCA (poly-crystalline alumina). PCA can withstand much higher temperatures, allowing the temperature of the discharge, wall and salt pool to be higher than for a discharge contained by a quartz burner. Therefore, more Dy is expected to be in the discharge in a PCA burner than is the case for burners made of quartz.

All measurements that were planned for micro-gravity conditions were duplicated during normal gravity conditions before the setup was sent to the ISS. Radial temperature profiles for a lamp containing 10 mg of Hg and 4 mg of DyI_3 are shown in figure 3.13 (a,b,c) for powers ranging from 110-150W. The figure shows that the arc contracts more strongly for 0- g ($\gamma = 1.8$ for 110W) than for 1- g ($\gamma = 1.2$ for 110W).

Radial atomic intensity profiles are plotted for 1- g and 0- g for different powers in figure 3.14(a,b,c). These profiles clearly indicate a shift in the distribution of Dy atoms at 0- g . For 0- g there is less atomic Dy in the centre of the discharge and more near the wall. This phenomenon can be explained by the absence of convection at 0- g . As there is no convection, there is no axial segregation. Assuming the cold spot temperature is roughly

¹The Hg ion density was calculated from the Hg atom density using Saha [11], where $n_e = n_{\text{Hg}^+}$

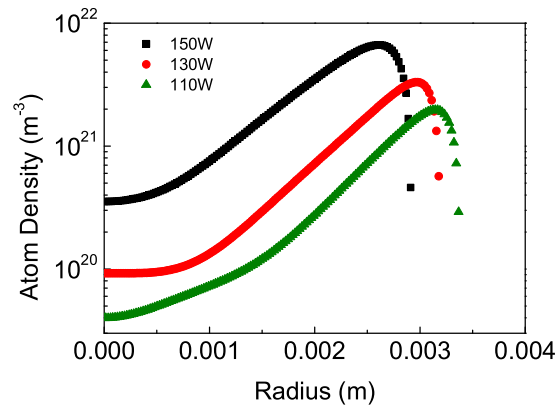


Figure 3.10: Radial density profile of atomic Dy at zero-*g* for a lamp containing 4 mg of DyI₃ and 10 mg of Hg.

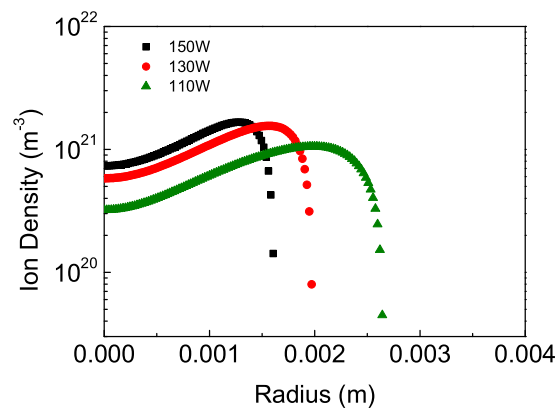


Figure 3.11: Radial density profile of ionic Dy at zero-*g* for a lamp containing 4 mg of DyI₃ and 10 mg of Hg.

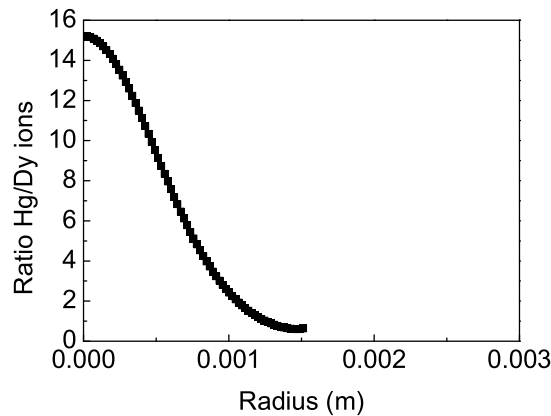


Figure 3.12: Ion ratio of Hg and Dy at zero- g for a lamp containing 4 mg of DyI_3 and 10 mg of Hg operated at 150 W.

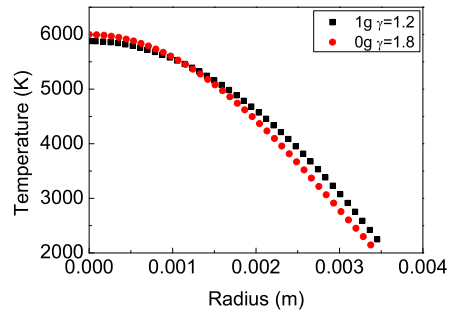
the same for 1- g as it is for 0- g , the absence of axial segregation at 0- g causes the Dy density to be distributed uniformly over the length of the lamp [5]. This results in an increase of Dy near the wall at the axial mid-point of the lamp. The stronger dip in the centre was caused by the increase of radial segregation as there is no mixing due to convection at 0- g . These effects cause the flank of the discharge to contain more Dy for 0- g than for 1- g , resulting in higher radiation loss at 0- g , leading to a stronger contraction at 0- g . The shift between 0- g and 1- g becomes less pronounced as the power increases. Both the temperature profiles and the intensity profiles show that at 150 W the discrepancy between 1- g and 0- g is diminished.

Scaled concentration profiles of the atomic density were calculated in order to eliminate temperature effects and the effects of axial segregation. The concentration was calculated by dividing the atom density by the total Hg density (acquired with $p = nkT$, assuming $T_{\text{eff}}=3000$ K). Then the 0- g concentration profile was scaled with the concentration profile of 1- g at 3 mm. The results are depicted in figure 3.15(a,b,c) for powers ranging from 110 to 150 W. As expected, more radial segregation occurs for 0- g than for 1- g , as there is no mixing due to convection in 0- g .

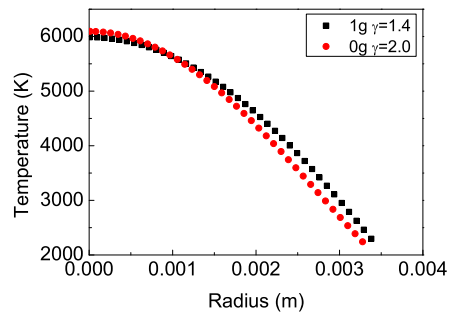
3.5 Conclusions

Absolute total atomic and ionic radial density profiles were constructed for lamps containing 10 mg of Hg and 4 mg of Dy under the micro-gravity conditions of the ISS. Radial density profiles of Dy show a clear separation between atomic and ionic regions in the plasma; the ionic region is in the hot centre, the atomic region surrounds it. Hg ions predominate in the centre of the discharge and contribute largely to the total electron density of the discharge.

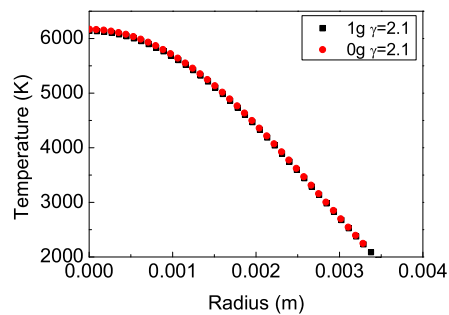
The radial temperature profiles were constructed from the lateral profile of atomic Hg



(a)

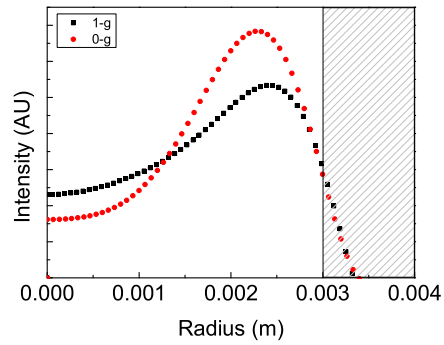


(b)

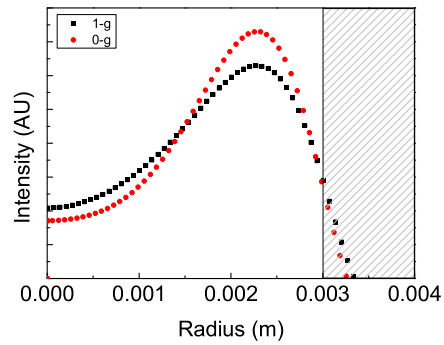


(c)

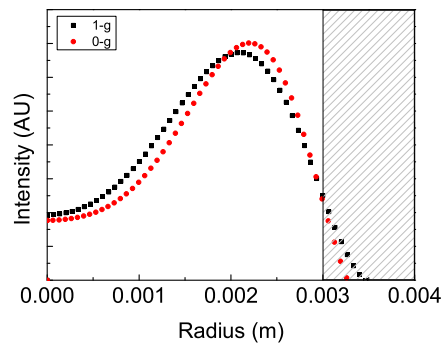
Figure 3.13: Radial temperature profiles for a lamp containing 4 mg of DyI_3 and 10 mg of Hg during normal and micro-gravity conditions at 110 W (a) 130 W (b) and 150 W (c). γ indicates the amount of contraction, $\gamma=1$ means there is no contraction. [10]



(a)

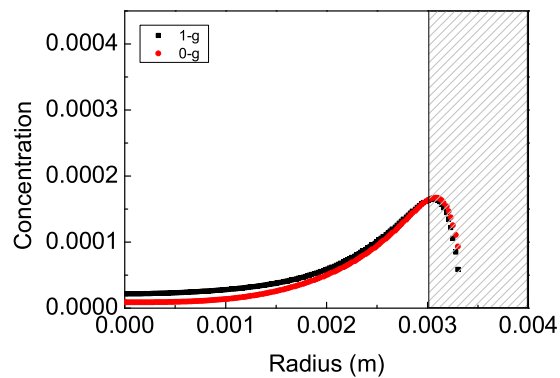


(b)

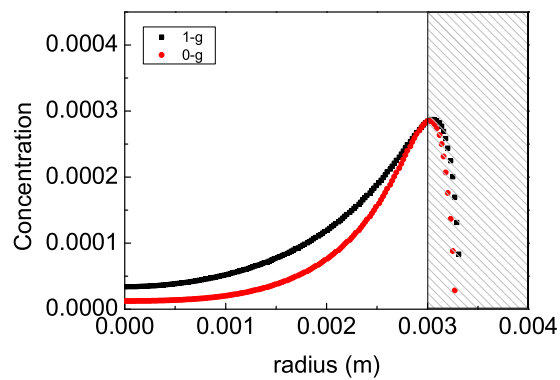


(c)

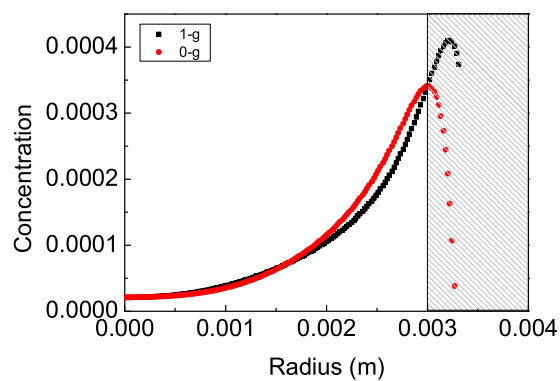
Figure 3.14: Intensity profile of atomic Dy for a lamp containing 4 mg of DyI_3 and 10 mg of Hg measured at normal and micro-gravity conditions for a lamp operated at 110 W (a) 130 W (b) and 150 W (c). The plots are considered to be reliable for $r < 3\text{mm}$, which is up to the shaded area.



(a)



(b)



(c)

Figure 3.15: Concentration profile of atomic Dy for a lamp containing 4 mg of DyI_3 and 10 mg of Hg measured at normal and micro-gravity conditions for a lamp operated at 110 W (a) 130 W (b) and 150 W (c). The plots are considered to be reliable for $r < 3\text{mm}$, which is up to the shaded area.

for different lamp powers. A lamp containing a pure Hg dose, operated at 150W, showed a temperature of 5800 K and a parabolic profile in the centre of the arc. The temperature profile of a lamp containing both Hg and Dy had a temperature of 6300 K at the axis of the lamp, in addition it showed a contracted profile, especially for higher powers.

Comparison between 0-*g* and 1-*g* showed, as expected, that there was more radial segregation at 0-*g*. The temperature profile of a lamp containing both Hg and Dy showed an axis temperature of 6100 K at 1-*g*, which is comparable to the axis temperature at 0-*g* within the error margin. The difference between 1-*g* and 0-*g* of the radial temperature, intensity and density profiles, decreased for high powers.

Absence of convection will facilitate the numerical study of the transport phenomena of the metal-halide lamp. Future study should include the comparison of the experimental results with the numerical model.

3.6 Acknowledgements

The authors wish to thank the ARGES team [22] [18], P.L.E.M. Pasmans and K.C. Kuiper for their contributions. The authors acknowledge the support from Philips Lighting, European Space Agency ESA, National Aerospace and Space Administration NASA, Russian Space Agency RSC Energia, SENTER, NOVEM, Space Research Organisation Netherlands SRON, the Netherlands Ministries for Education and Research and for Economic affairs, the executive board of the Eindhoven University of Technology, and Technologiestichting STW (project ETF. 6093), COST (project 529).

Bibliography

- [1] Lister G G, Lawler J E, Lapatovich W P and Godyak V A 2004 Rev. Mod. Phys. **76**, 541
- [2] Fischer E 1976 J. Appl. Phys. **47**, 2954
- [3] Bellows A H, Feuersanger A E, Rogoff G L, and Rothwell H L 1984 *HID convection studies: a space shuttle experiment* Illuminating Engineering Soc. Meeting
- [4] Bellows A H, Feuersanger A E, Rogoff G L, and Rothwell H L 1984 *Convection and Additive segregation in High pressure lamp arcs: Early results from a space shuttle experiment* Gaseous electronics Conf., 1985 Bull. Amer. Phys. Soc. Vol **30**, p 141
- [5] Flikweert A J, Van Kemenade M, Nimalasuriya T, Haverlag M, Kroesen G M W and Stoffels WW 2006 J.Phys.D **39**, 1599
- [6] Stoffels W W, Haverlag M, Kemps P C M, Beckers J and Kroesen G M W 2005 Appl. Phys. Lett. **87** 1
- [7] Nimalasuriya T, Pupat N B M, Flikweert A J, Stoffels W W, Haverlag M and Van der Mullen J J A M 2006 J. Appl. Phys. **99** 053302 **see chapter 2**
- [8] Zhu X 2005 Ph.D. thesis *Active spectroscopy on HID lamps*, Eindhoven University of Technology
- [9] Elenbaas W 1951 *The high pressure mercury vapour discharge*, 1st ed., (North-Holland publishing company)
- [10] Fischer E 1978 *Influences of External and Self-Magnetic Fields on the behaviour of discharge lamps*, Philips GmbH Forschungslaboratorium Aachen Lobornotiz nr 13/78.
- [11] Mitchner M and Kruger Jr C H 1973 *Partially ionized gases*, 1st ed., (John Wiley and Sons).
- [12] Kurucz R L and Bell B 1993 *Atomic Line Data CD-ROM No 23* (Cambridge, MA: Smithsonian Astrophysical Observatory)
- [13] Wickliffe M W and Lawler J E 2000 J. Quant. Spectrosc. Radiat. Transfer **66**, 363
- [14] http://www.thespectroscopynet.com/Theory/Partition_Functions.asp
- [15] Curry J J, Sakai M and Lawler J E 1998 J. Appl. Phys. **84**, 3066
- [16] Flikweert A J, Nimalasuriya T, Groothuis C H J M, Kroesen G M W and Stoffels W W 2005, J. Appl. Phys. **98** 073301
- [17] Kemps P C M, 2004 Master's thesis *An experimental study of the radial additive density and plasma temperature profiles, and the effect of this on the integral light output of metal halide lamps as a function of gravity* Eindhoven University of Technology

- [18] Kroesen G M W, Haverlag M, Dekkers E, Moerel J, de Kluijver R, Brinkgreve P, Groothuis C H J M, Van der Mullen J J A M, Stoffels W W, Keijser R, Bax M, Van den Akker D, Schiffeleers G, Kemps P C M, Van den Hout F H J, Kuipers A 2005 Microgravity sci. technol. XVI-1
- [19] Nimalasuriya T, Thube G M, Flikweert A J, Haverlag M, Kroesen G M W and Stoffels W W 2007 J.Phys.D 40, 2839 **see chapter 3**
- [20] Benck E C, Lawler J E and Dakin J T 1989 J. Opt. Soc. Am. B **6**, 11
- [21] Van der Mullen J J A M 1990 Phys. Rep. **191** 109
- [22] Stoffels W W, Kroesen G M W, Groothuis C H J Mv, Flikweert A J, Nimalasuriya T, Van Kemenade M, Kemps P C M, Bax M, Van den Hout F H J, Van den Akker D, Schiffelers G, Beckers J, Dekkers E, Moerel J, Brinkgreve P, Haverlag M, Keijser R and Kuipers A 2005 Proceedings of the XXVIIth International Conference on Phenomena in Ionised Gases Eindhoven (16-342), july 17-22, 2005, E.M. Van Veldhuizen, Eindhoven University of Technology.